

Received June 15, 2017, accepted July 15, 2017, date of publication July 24, 2017, date of current version August 14, 2017.

Digital Object Identifier 10.1109/ACCESS.2017.2730850

Learning Automata-Based Methodology for Optimal Allocation of Renewable Distributed Generation Considering Network Reconfiguration

JUNPENG ZHU¹, WEI GU¹, (Senior Member, IEEE), GUANNAN LOU¹, LIUFANG WANG², BIN XU², MING WU³, AND WANXING SHENG³

¹School of Electrical Engineering, Southeast University, Nanjing 210096, China

²State Grid Anhui Electric Power Corporation Research Institute, Hefei 230000, China

³China Electric Power Research Institute, Beijing 100192, China

Corresponding author: Wei Gu (wgu@seu.edu.cn)

This work was supported by the State Grid Corporation of China under Grant SGTYHT/15-JS-191.

ABSTRACT The inadequate capacity of distribution networks to consume renewable energy and the inappropriate allocation of renewable distributed generation (RDG) have become important issues. In this paper, a 3-level learning automata-based methodology in a master—slave structure is proposed for optimal RDG siting and sizing considering network reconfiguration. The RDG allocation optimization, i.e., the master problem, is proposed in the first level, with the objective of minimizing the annual investment cost and operation cost. Network reconfiguration is modeled as a slave problem in the second level to promote the consumption of RDG and decrease the operation cost. The RDG power control strategy, including active power curtailment and reactive power compensation, is introduced as a secondary slave problem in the third level. Considering the stochastic characteristics of renewable energy and loads, intelligent algorithms based on learning automata are proposed and embedded into the master—slave structure. The simulation results on the standard test systems demonstrate the feasibility and effectiveness of proposed method.

INDEX TERMS Distributed generation allocation, network reconfiguration, learning automata, renewable energy, active distribution network.

ABBREVIATIONS

| | |
|------|---|
| DG | Distributed generation |
| RDG | Renewable distributed generation |
| PV | Photovoltaic |
| FL | Fundamental loop |
| LA | Learning automata |
| CALA | Continuous action-set learning automata |
| FALA | Finite action-set learning automata |
| PSO | Particle swarm optimization |

INDEXES

| | |
|-----------|---------------------------------|
| t | Index for time |
| y | Index for year |
| s | Index for scenario |
| i, j | Index for node |
| φ | Index for equality constraint |
| ψ | Index for inequality constraint |

OBJECTIVES

| | |
|-------------|--|
| C_{total} | Total annual cost |
| C_{inv} | Annual investment cost |
| C_{ope} | Annual operation and maintenance cost |
| C_{uti}^y | Electricity purchasing cost in the y^{th} year |
| C_{om}^y | RDG operation and maintenance cost in the y^{th} year |
| C_{rec}^y | Switch operation cost in the y^{th} year |
| C_{SUB}^y | Economic compensation of the renewables in the y^{th} year |

CONTROL VARIABLES

| | |
|----------------|--|
| χ_{allo} | Control variable of RDG allocation |
| χ_{conf} | Control variable of network reconfiguration |
| χ_{power} | Control variable of RDG output power |
| $\chi_{i,loc}$ | Control variable of RDG location in node i |
| Cap_i | Control variable of RDG capacity in node i |

| | |
|------------|--|
| CV | Configuration vector |
| $P_{i,DG}$ | Active output power of RDG in node i |
| $Q_{i,DG}$ | Reactive output power of RDG in node i |

SETS

| | |
|-----------------|---|
| Ω_{cand} | Set of RDG candidate nodes |
| Ω_s | Set of typical scenarios |
| $u(j)$ | Set of sending ends of the lines with node j as the receiving end |
| $v(j)$ | Set of receiving ends of the lines with node j as the sending end |

PARAMETERS

| | |
|--------------------|---|
| $C_{inv,fix}$ | Fixed cost of the RDG station |
| $C_{inv,mar}$ | Marginal cost of the RDG station |
| C_{om} | RDG operation and maintenance price |
| C_{rec} | Cost of single switch operation |
| C_{uti} | Electricity price |
| C_{sub} | Compensation price |
| Cap_i^{max} | Maximum RDG capacity in node i |
| N_{DG}^{max} | Maximum RDG amount |
| N_{Switch}^{max} | Upper limit of the switch operation times |
| U_{min} | Upper limit of the voltage magnitude |
| U_{max} | Lower limit of the voltage magnitude |
| η | Coefficient of renewable energy |
| $N_{iteration}$ | Maximum iterations |
| r | Inflation rate |
| N_d^s | Occurrence number of scenario s in a year |

OTHER VARIABLES

| | |
|--------------------|--|
| A | Bus incidence matrix of the network |
| U_i | Voltage magnitude in node i |
| N | Normal distribution |
| β | Response of the environment in FALA |
| P_n | Action probability vector in FALA |
| $best$ | Current optimal value in FALA |
| f_{obj} | Objective function in FALA |
| P_{ij} | Active power of the sending end of line ij |
| Q_{ij} | Reactive power of the sending end of line ij |
| $P_{i,L}$ | Active power of the load in node i |
| $Q_{i,L}$ | Reactive power of the load in node i |
| N_{sw}^s | Number of switch operations in scenario s |
| P_{uti} | Injected active power from the transmission system |
| $C_{ope,opt}$ | Annual operation cost determined in the second level |
| $\chi_{power,opt}$ | RDG output power determined in the third level |
| $flag_{ope}$ | Operation constraint flag |
| $flag_{control}$ | Control constraint flag |
| η_{exp} | Expected value of renewable energy * coefficient |
| $P_{i,exp}$ | Expected value of active load in node i |
| $Q_{i,exp}$ | Expected value of reactive load in node i |

| | |
|-----------------|--|
| σ_{DG} , | Standard deviation of renewable energy coefficient |
| $\sigma_{i,P}$ | Standard deviation of active load in node i |
| $\sigma_{i,Q}$ | Standard deviation of reactive load in node i |

I. INTRODUCTION

The penetration of renewable energy and distributed generation has been increasing in last decades. According to the government report from National Energy Administration of China, by the end of 2015 the installed capacity of renewable energy in China is more than 480 million kW. The electricity generated by the renewable energy is about 1363 billion kW·h, providing for 24.5% of total electricity consumption. In Yunnan and Sichuan Provinces, this proportion of electricity generated by renewable energy has reached about 80%. However, the curtailment situation of the renewable energy is serious. In Gansu and Xinjiang Provinces, the curtailment rates of photovoltaic power are 31% and 26% respectively. In Xinjiang and Jilin Provinces, the curtailment rates of wind power have reached 32%. The rational allocation of renewable distributed generation (RDG) and the assistant operation strategy of electrical power systems are two important ways to mitigate this issue. For this purpose, an optimal RDG siting and sizing method considering the network reconfiguration technology is studied in this paper.

Optimal siting and sizing of distributed generations (DGs) considering various technical concerns has been discussed considerably over the last decade [1]–[9]. In [1], an analytical approach for optimal siting and sizing of distributed generation in radial power distribution networks to minimize power loss is presented. A cost based DG sizing and siting strategy is proposed considering the direct and indirect costs of DG investment, total power operation, power supply quality, reliability and energy loss in [2]. Reliability criteria are also considered in DG siting and sizing model in [3] and [4]. Stochastic models are proposed for optimal DG sitting and sizing in [5]–[7]. The uncertain load growth and the uncertain output power of plug-in electric vehicles, wind generation unit and solar generating source are considered in [5]. In [6], reactive power allocation is optimized together with DG siting and sizing, and the stochastic characteristics of wind and solar energy are taken into consideration. The DG sitting and sizing problem has been formulated as multi-objective optimization models in [8] and [9]. In [8], the operation of power quality indicators like voltage quality and harmonic distortion is also considered in the network performance, and a double trade-off procedure is introduced to solve the model. In [9], the cost of network upgrading, power losses, energy not supplied and energy required by the served customers are considered, and the model is solved by a genetic algorithm embedded with a ε -constrained method.

Previous work has studied the benefit of network reconfiguration on reducing power loss [10], maintaining power balance [11], promoting voltage condition [12], reducing activity cost of DISCOs [13], and the combination of them [14]. With increasing penetration levels of distributed energy resources,

the benefit of network reconfiguration to help integrate RDG has also drawn attention from researchers [15]–[18]. Ref. [15] established an active distribution system reconfiguration model, the objective of which is to maximize the overall amount of RDG that can be hosted by the distribution system. The results show that the application of static or dynamic reconfiguration is an effective method to accommodate larger amounts of RDG in distribution systems without network reinforcement. The work in [16] shows that after reconfiguration, the maximum capacity of RDG that the system could absorb can be increased by about 102% in a standard test system. Ref. [17] shows that reconfiguration can reduce the curtailment of RDG. The study in [18] also demonstrates that hourly reconfiguration not only decreased electrical losses, but also released more free capacity for RDG. However, the works in [15]–[18] are not proposed from the point of RDG planning: the technical feasibility to help consume renewables by network reconfiguration has been demonstrated, but the economic feasibility and advantages have not been studied. The investment cost of RDG and the operation cost of RDG and switches are not considered in [15]–[18].

In recent years, some of the DG siting and sizing research has considered the effect of the network configuration [19]–[26], however, in most of these research the DG is not particularly referred as RDG and the characteristics of renewable energy have not been discussed [19]–[23]. In [19]–[23], the objective is to optimize the network operation status (e.g., reduce the power loss and improve the voltage profile) instead of promoting the DG penetration. The DGs are more expected as the auxiliary element in power system for better operation status than the energy resource. Therefore, the investment and operation cost of DGs are not considered in [19]–[23]. In [24]–[26] the RDG are taken into consideration. In [24] a simultaneous model of reconfiguration and optimal allocation of photovoltaic (PV) arrays and distribution static compensator is proposed. Ref. [25] proposed a simultaneous model of RDG allocation, network reconfiguration and expansion planning to meet the load rise with minimum cost and acceptable quality standards. A multi-objective model is proposed in [26] to handle the simultaneous RDG allocation and reconfiguration problem, in which pollutant gas emission is also considered as one of the objectives. However, in [24]–[26] only static reconfiguration is considered and the benefit of dynamic network reconfiguration has not been studied.

This paper proposes a 3-level RDG siting and sizing model considering dynamic network reconfiguration and stochastic nature of renewable energy. Compared with previous work, the innovations of this work are as follows:

(1) In previous RDG siting and sizing research, the RDG power control, including RDG power curtailment, has been considered to satisfy the network constraint or achieve higher network performance, while the dynamic network reconfiguration which might be a more economic strategy to achieve the same effect has not been considered. In this paper a novel

optimal RDG siting and sizing model considering dynamic network reconfiguration and RDG control strategy is proposed.

(2) Previous work has discussed the benefit of network reconfiguration to help integrate renewables technically, but the economic benefit has rarely been analyzed. The paper gives an economic quantitative evaluation of the benefit of network reconfiguration on RDG penetration.

(3) A 3-level master–slave structure embedded with learning automata based algorithms is proposed for the simultaneous model of RDG allocation and reconfiguration. The stochastic characteristics of RDG and load can be considered in the learning automata. In the master–slave structure the RDG allocation and network reconfiguration are optimized separately, which can reduce the dimensionality of solution space and improve the solving accuracy and efficiency.

The remainder of this paper is organized as follows. The 3-level optimal RDG siting and sizing model is proposed in Section II, the learning automata based algorithms and strategies are proposed in Section III, case studies are presented in Section IV, and Section V concludes the paper.

II. MODELING OF OPTIMAL SITING AND SIZING OF RDG CONSIDERING NETWORK RECONFIGURATION

A. THE 3-LEVEL MASTER–SLAVE STRUCTURE OF THE MODEL

The RDG siting and sizing model considering network reconfiguration can be expressed abstractly:

$$\text{Min}_{\chi_{allo}, \chi_{conf}, \chi_{power}} C_{total} \quad (1)$$

$$\varphi(\chi_{allo}, \chi_{conf}, \chi_{power}) = 0 \quad (2)$$

$$\psi(\chi_{allo}, \chi_{conf}, \chi_{power}) \leq 0 \quad (3)$$

C_{total} is the total annual cost. χ_{allo} , χ_{conf} , and χ_{power} are the control variables of RDG allocation (siting and sizing), network reconfiguration and RDG output power respectively. φ and ψ are the equality constraint and inequality constraint respectively.

Eq. (1)–(3) describe a simultaneous model with coupled control variables, which is very difficult to solve. Referring to the construction and operation of actual power system, the process can be divided into 3 stages generally: planning stage, operation stage (day-ahead dispatch) and real-time control stage. During each stage the optimizing objective and constraints are different. Based on this consideration, the model (1)–(3) can also be expressed as:

$$\begin{aligned} \text{Min}_{\chi_{allo}, \chi_{conf}, \chi_{power}} C_{total} = & C_{inv}(\chi_{allo}) \\ & + C_{ope}(\chi_{allo}, \chi_{conf}, \chi_{power}) \end{aligned} \quad (4)$$

$$\varphi_{plan}(\chi_{allo}) = 0 \quad (5)$$

$$\psi_{plan}(\chi_{allo}) \leq 0 \quad (6)$$

$$\varphi_{ope}(\chi_{allo}, \chi_{conf}) = 0 \quad (7)$$

$$\psi_{ope}(\chi_{allo}, \chi_{conf}) \leq 0 \quad (8)$$

$$\varphi_{control}(\chi_{allo}, \chi_{conf}, \chi_{power}) = 0 \tag{9}$$

$$\psi_{control}(\chi_{allo}, \chi_{conf}, \chi_{power}) \leq 0 \tag{10}$$

In Eq. (4), the total cost includes two parts: the investment cost C_{inv} , the operation and maintenance cost C_{ope} . C_{inv} can be calculated by the RDG allocation in the planning stage, while C_{ope} needs the operation status. Eq. (5)-(6) represent the constraints in the planning stage and only RDG capacity and location variables are involved. Eq. (7)-(8) represent the constraints of network reconfiguration in the operation stage. When the RDG is penetrated, the network reconfiguration schedule is effected by the allocation. Eq. (9)-(10) represent the constraints in RDG power control process, including the power flow and system safety constraints.

Based on (4)-(10), the model can be divided into several sub-problems in a multi-level iterative master—slave structure, seen in Fig. 1.

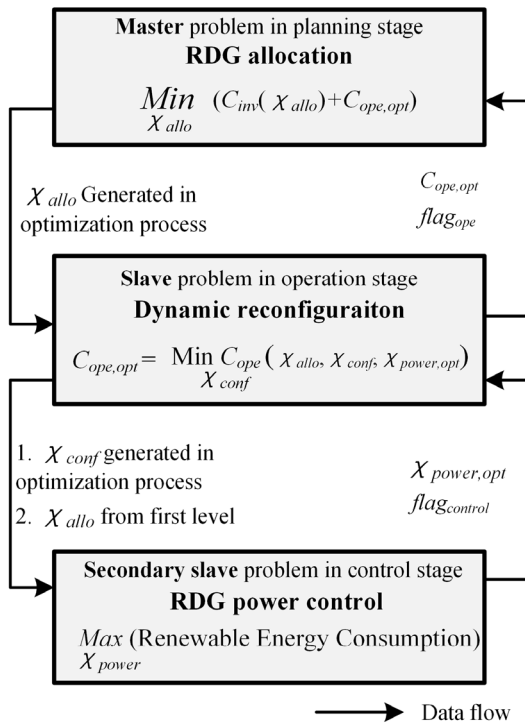


FIGURE 1. Master—slave structure of the RDG siting and sizing model.

In Fig. 1, $C_{ope,opt}$ is the annual operation cost, which is the optimization result of the second level model. Meanwhile, it is the feedback of χ_{allo} generated in the master problem. $\chi_{power,opt}$ is the RDG power determined in the third level. $flag_{ope}$ and $flag_{control}$ are the constraint flags from the second and third level models respectively.

The master problem is proposed in the first level, corresponding to the planning stage optimization. The control variable only includes χ_{allo} . This model is solved by a learning automata based algorithm proposed in Section III. For each intermediate control variables generated in the optimization process, the fitness value, i.e., the total annual cost, should

be calculated. C_{ope} cannot be determined directly by χ_{allo} , so a slave problem is proposed in the second level, corresponding to the operation stage optimization, to reduce and finally determine the operation cost $C_{ope,opt}$.

Network reconfiguration, which can promote RDG power consumption, is considered as the main technique in the second level. In this level, the dynamic reconfiguration schedule χ_{conf} is the only control variable, and the optimization model is also solved by a learning automata based algorithm proposed in Section III. To determine the RDG power under each reconfiguration schedule generated in the optimization process, a secondary slave problem is proposed in the third level, i.e., the RDG power control strategy. RDG active power curtailment and reactive power compensation strategies are proposed in this level for maximum renewable energy consumption.

The detailed models in 3 levels are given in the rest of this section.

B. MASTER PROBLEM: RDG ALLOCATION OPTIMIZATION

1) ABSTRACT FORMULATION

The master problem is formulated abstractly as:

$$C_{total} = \text{Min}_{\chi_{allo}} (C_{inv}(\chi_{allo}) + C_{ope,opt}) \tag{11}$$

subject to:

$$flag_{ope} = 1 \tag{12}$$

Eq.(5) – (6)

where, $C_{ope,opt}$ is the feedback of χ_{allo} from the operation stage optimization in the second level, which can be considered as an implicit function of χ_{allo} . Eq. (12) ensures that for a feasible RDG allocation, the constraints in the operation stage can be satisfied. Since the operation stage is also formulated as an optimization model, Eq. (12) can be described as: there exist at least one operation solution (reconfiguration schedule) in the operation stage such that the constraints in the second level can be all satisfied.

2) CONTROL VARIABLE ENCODING

χ_{allo} includes the information of RDG location and capacity:

$$\chi_{allo} = [x_{1,loc}, Cap_1, x_{2,loc}, Cap_2, \dots, x_{i,loc}, Cap_i, \dots, x_{Ncand,loc}, Cap_{Ncand}] \tag{13}$$

where, $x_{i,loc}$ and Cap_i are the control variables of candidate node i . $x_{i,loc} = 1$ if there is an RDG in candidate node i and $x_{i,loc} = 0$ if there isn't. Cap_i is the capacity of the RDG in candidate node i .

3) DETAILED FORMULATION

Based on the encoding, the investment cost can be calculated by Eq. (14)-(15):

$$C_{inv}(\chi_{allo}) = \sum_{y=1}^y \frac{1}{(1+r)^y} C_{inv}^y(\chi_{allo}) \tag{14}$$

$$C_{inv}^y(\chi_{allo}) = \begin{cases} \sum_{i \in \Omega_{Cand}} x_{i,loc} \cdot (c_{inv,fix} + c_{inv,mar} \cdot Cap_i) & y = 1 \\ 0 & y \geq 2 \end{cases} \quad (15)$$

where, Y is the planning cycle (for years), r is the inflation rate. C_{inv}^y is the RDG investment cost incurs in the y^{th} year. $c_{inv,fix}$ and $c_{inv,mar}$ are fixed cost and marginal cost of the RDG station. Ω_{cand} is the set of RDG candidate nodes, $|\Omega_{cand}| = N_{cand}$.

The constraints Eq. (5)-(6) can be explicitly expressed as:

$$x_{i,loc} \cdot (x_{i,loc} - 1) = 0 \quad (16)$$

$$Cap_i \leq x_{i,loc} \cdot Cap_i^{max} \quad (17)$$

$$\sum_{i \in \Omega_{Cand}} x_{i,loc} \leq N_{DG}^{max} \quad (18)$$

where, Cap_i^{max} is the maximum RDG capacity in node i , N_{DG}^{max} is the maximum amount of RDG stations.

4) ALGORITHM

The master problem (Eq. (11)-(12), (14)-(18)) is solved by the learning automata (LA) based algorithm introduced in Section III.

C. SLAVE PROBLEM: NETWORK DYNAMIC RECONFIGURATION

1) ABSTRACT FORMULATION

The slave problem aims to minimize the operation cost for a given RDG allocation, which can be formulated abstractly as:

$$C_{ope,opt} = \underset{\chi_{conf}}{Min} C_{ope}(\chi_{allo}, \chi_{conf}, \chi_{power,opt}) \quad (19)$$

subject to:

$$flag_{control} = 1 \quad Eq.(7) - (8) \quad (20)$$

In this level, χ_{allo} is constant, and $\chi_{power,opt}$ can also be considered as an implicit function of χ_{conf} , because it's the feedback of χ_{conf} in the secondary slave model, seen in Fig. 1. The reconfiguration schedule χ_{conf} is the only control variable in this stage. Eq. (20) ensures that for a feasible reconfiguration schedule, there exist an RDG power control strategy such that the constraints in the third level can be all satisfied.

2) CONTROL VARIABLE ENCODING

The distribution network is reconfigured by opening/closing sectionalizing-switches and tie-switches. The reconfiguration can be treated as a "1" and "0" combinatorial optimization of the switches. In this paper it is assumed that all the feeders are equipped with remote switches. The fundamental loops (FLs) are determined for the meshed network by closing all tie-switches, seen in Fig. 2 as an example.

To preserve the radial structure of the network, there is at least one switch open in each FL. On the other hand,

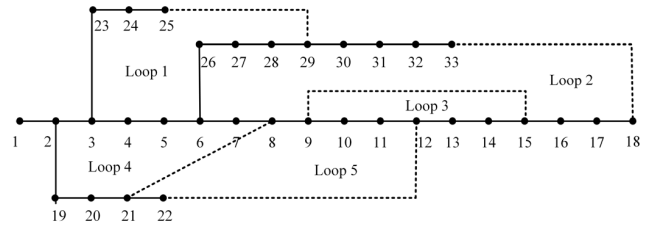


FIGURE 2. FLs in the 33-bus distribution system [27].

according to graph theory [28], the number of open switches in a radial structure is equal to the number of tie-switches, which is equal to the number of FLs, too. So we can draw the conclusion that all the feasible radial structures could be formed through opening one switches from each FL respectively. The encoding strategy is to use a number to represent the opening switch in each FL. For example, configuration vector [8, 13, 7, 7, 2] represents a feasible structure with the 8th, 13th, 7th, 7th, 2nd switch in the 1-5 FLs respectively.

The annual operation cost C_{ope} is calculated based on daily operation cost in typical scenarios. The control variable χ_{conf} includes the hourly reconfiguration schedule of each daily scenario, which needs 24 configuration vectors to represent the network structure in each hour. The encoding of χ_{conf} is:

$$\chi_{conf} = [\underbrace{CV^{1,1} - CV^{24,1}}_{Scenario\ 1}, \dots, \underbrace{CV^{1,s} - CV^{24,s}}_{Scenario\ s}, \dots, \underbrace{CV^{1,Ns} - CV^{24,Ns}}_{Scenario\ Ns}] \quad (21)$$

$CV^{t,s}$ is the configuration vector of time t in scenario s . Ns is the number of scenarios.

Some notes about the encoding should be given:

(1) There is a simplification of the reconfiguration model in the encoding strategy. The main effect of network reconfiguration is to balance the load rate between feeders and to improve the voltage profile. The minor growth of the loads will not significantly influence the load rates of the feeders or the system voltage condition, so the network reconfiguration schedule in each scenario are not changed by years. This simplification can considerably reduce the dimensionality of the control variable.

(2) All the feasible structures can be represented by the FL encoding strategy, but not all of the configuration vectors correspond to a feasible structure because the FLs have public feeders. For example, if the switch 26-27 is opened in FL1 and switch 28-29 is opened in FL2, then nodes 27 and 28 are isolated. So the structure constraints should be contained in Eq. (7)-(8).

3) DETAILED FORMULATION

C_{ope} is calculated by Eq. (22)-(26):

$$C_{ope} = \sum_{y=1}^Y \frac{1}{(1+r)^y} (C_{om}^y + C_{rec}^y + C_{uti}^y - C_{sub}^y) \quad (22)$$

$$C_{om}^y = \sum_{i \in \Omega_{Cand}} x_{i,loc} \cdot c_{om} \cdot Cap_i \quad (23)$$

$$C_{rec}^y = \sum_{s \in \Omega_s} N_d^s \cdot N_{sw}^s \cdot c_{rec} \quad (24)$$

$$C_{uti}^y = \sum_{s \in \Omega_s} \sum_{t=1}^{24} N_d^s \cdot c_{uti}^t \cdot P_{uti}^{t,s,y} \quad (25)$$

$$C_{sub}^y = \sum_{s \in \Omega_s} \sum_{i \in \Omega_{Cand}} \sum_{t=1}^{24} N_d^s \cdot x_{i,loc} \cdot c_{sub} \cdot P_{i,DG}^{t,s,y} \quad (26)$$

where, t , s and y are the symbols of time, scenario and year respectively. C_{om}^y , C_{rec}^y , C_{uti}^y are the RDG operation and maintenance cost, switch operation cost, electricity purchasing cost in the y^{th} year. According to the government policy, the compensation of the renewables C_{sub}^y is also considered in the economic evaluation. c_{om} is the operation and maintenance price of RDG per capacity, c_{rec} is the cost of single switch operation, c_{uti} and c_{sub} are the electricity price and compensation price, respectively. Ω_s is the set of typical scenarios, $|\Omega_s| = N_s$. N_d^s is the occurrence number of scenario s in a year. N_{sw}^s is the number of switch operations in scenario s , $P_{uti}^{t,s,y}$ and $P_{i,DG}^{t,s,y}$ are the injected active power from the transmission system and the RDG active output in time t , scenario s and year y .

In Eq. (23), C_{om}^y is a function of χ_{allo} because the operation and maintenance cost of RDG is considered to be proportional to the RDG capacity. In Eq. (24), C_{rec}^y is a function of χ_{conf} because N_{sw}^s is determined by the dynamic reconfiguration schedule. In Eq. (26) and (25), C_{sub}^y and C_{uti}^y are the functions of $\chi_{power,opt}$ because $P_{i,DG}^{t,s,y}$ is the RDG active power determined in the third level, i.e., $P_{i,DG}^{t,s,y}$ is a part of $\chi_{power,opt}$, and the injected active power from the transmission system $P_{uti}^{t,s,y}$ is determined by the output of RDG, i.e., is determined by $\chi_{power,opt}$:

$$P_{uti} = \sum_j (P_{j,L} + \sum_{i \in u(j)} (\frac{(P_{ij})^2 + (Q_{ij})^2}{(U_i)^2} r_{ij}) - P_{j,DG}) \forall t, s, y \quad (27)$$

where, $P_{j,L}$ is the active load in node j . $u(j)$ is the set of sending ends of the lines which have node j as the receiving end, P_{ij} is the active power of the sending end of line ij .

The constraints (7)-(8) include the structure radiality constraint and switch operation frequency constraint:

$$\det(A) = 1 \text{ or } -1 \quad (28)$$

$$N_{sw}^s \leq N_{Switch}^{max} \quad (29)$$

where, A is the bus incidence matrix of the network which can be determined by the configuration vector. This constraint should be satisfied at any time in each scenario. N_{Switch}^{max} is the upper limit of the switch operation times.

4) ALGORITHM

The dynamic reconfiguration problem (Eq. (19)-(20), (22)-(29)) is solved by the learning automata based algorithm introduced in Section III.

D. SUB-SLAVE PROBLEM: RDG POWER CONTROL

1) ABSTRACT FORMULATION

The output power of RDG is non-completely controllable: the maximum active power is effected by the environment (e.g., wind speed and light intensity). Generally the RDG operates under the MPPT mode for renewable energy consumption and economic benefit. The active output power can be curtailed from the maximum value and some of the RDG has the capability of reactive power compensation. In this level, the RDG power control strategy aims to maximize the renewable energy consumption, and both power curtailment and reactive power compensation are considered to satisfy the system operation constraints.

$$\text{Max} (R \text{ renewableEnergy Consumption}) \quad (30)$$

χ_{power}

subject to:

$$Eq.(9) - (10)$$

where, χ_{allo} and χ_{conf} are constant in this level. The control variable χ_{power} includes $P_{i,DG}^{t,s,y}$ and $Q_{i,DG}^{t,s,y}$ for each candidate node i , time t , scenario s and year y . The optimization result of χ_{power} is denoted as $\chi_{power,opt}$.

2) DETAILED FORMULATION

The constraints (9)-(10) can be explicitly expressed by (31)-(36). The constraints should be satisfied for any time t , scenario s and year y , so the symbols are omitted for easy reading.

$$\sum_{i \in u(j)} (P_{ij} - \frac{(P_{ij})^2 + (Q_{ij})^2}{(U_i)^2} r_{ij}) + P_{j,DG} + P_{j,uti} - P_{j,L} = \sum_{k \in v(j)} P_{jk} \quad (31)$$

$$\sum_{i \in u(j)} (Q_{ij} - \frac{(P_{ij})^2 + (Q_{ij})^2}{(U_i)^2} x_{ij}) + Q_{j,DG} + Q_{j,uti} - Q_{j,L} = \sum_{k \in v(j)} Q_{jk} \quad (32)$$

$$(U_j)^2 = (U_i)^2 - 2(r_{ij}P_{ij} + x_{ij}Q_{ij}) + ((r_{ij})^2 + (x_{ij})^2) \frac{(P_{ij})^2 + (Q_{ij})^2}{(U_i)^2} \quad (33)$$

$$P_{i,DG} \leq Cap_i \cdot \eta \quad (34)$$

$$(P_{i,DG})^2 + (Q_{i,DG})^2 \leq (Cap_i)^2 \quad (35)$$

$$U_{min} \leq U_i \leq U_{max} \quad (36)$$

where, $u(j)$ is the set of sending ends of the lines which have node j as the receiving end, $v(j)$ is the set of receiving ends

of the lines which have node j as the sending end. If j is the substation node, $P_{j,uti} = P_{uti}$ and $Q_{j,uti} = Q_{uti}$, otherwise $P_{j,uti} = Q_{j,uti} = 0$. P_{ij} and Q_{ij} are the active power and reactive power of the sending end of line ij respectively, P_i and Q_i are the net active and reactive power injection in node i . $P_{i,L}$ and $Q_{i,L}$ are the active and reactive power of the load in node i respectively. η is the coefficient of renewable energy determined by the environment, which varies by the time t and scenario s . U_i is the voltage magnitude in node i , U_{min} and U_{max} are the upper and lower limits of the voltage magnitude respectively.

Eq. (31)-(33) are the distribution network Disflow equations, Eq. (34)-(35) are the RDG power constraints, Eq. (36) is the voltage constraint.

3) STRATEGY

The RDG power control strategy is given in Section III.

E. STOCHASTIC MODEL OF RENEWABLE ENERGY AND LOADS

The normal distribution is applied to describe the stochastic characteristics of renewable energy and loads:

$$\eta \sim N(\eta_{exp}, \sigma_{DG}) \quad \forall t, s, y \quad (37)$$

$$P_{i,L} \sim N(P_{i,exp}, \sigma_{i,P}) \quad \forall t, s, y \quad (38)$$

$$Q_{i,L} \sim N(Q_{i,exp}, \sigma_{i,Q}) \quad \forall t, s, y \quad (39)$$

where, η_{exp} , $P_{i,exp}$ and $Q_{i,exp}$ are the expected values of renewable energy coefficient, active load and reactive load respectively. σ_{DG} , $\sigma_{i,P}$ and $\sigma_{i,Q}$ are the standard deviations.

III. ALGORITHM AND STRATEGIES

In the 3-level structure, the master, slave and secondary slave problems are all formulated as optimization models. The learning automata based algorithms, which can deal with the stochastic environment, are proposed to solve the master and slave problems. The RDG power in sub-slave problem is determined by a fast and efficient strategy based on MPPT considering the computation complexity of the entire problem and the real-time requirement in actual power systems.

A. LA BASED ALGORITHMS FOR MASTER AND SLAVE PROBLEMS

Adaptive learning algorithms are efficient for optimization and control in complex no-linear systems [29], [30]. Learning automata are adaptive decision makers that learn to choose the optimal solution from the feasible region by using noisy reinforcement feedback from the stochastic environment [31]. The goal of LA is to find the optimal solution, where the expectation of the feedback from the stochastic environment is minimized. In the LA based algorithm, the value in each dimension of the control variable is set to obey a hypothetical probability distribution. At each iteration, the control variable is randomly selected according to the distributions, and the environment variable is also generated randomly based on its stochastic characteristics.

The reinforcement of the control variable distribution is obtained from the environment. The iteration ends when the state, where the probability of choosing the optimal set of actions is high enough, is evolved.

LA can be divided into CALA (continuous action-set learning automata) and FALA (finite action-set learning automata) according to whether the control variable is continuous or discrete. In proposed model, χ_{allo} and χ_{conf} are all discrete variables, so only the FALA based algorithm is introduced in this paper.

For finite decision variables, the feasible region is formed by limited areas. The decision variables are assumed to obey a discrete probability distribution in the feasible region. Denote the finite control variables as χ and the environment stochastic variables as ξ . The flow of the FALA based algorithms are as follows:

(1) Step 1: $n=1$. Initialize the probability distributions of decision variable χ . Suppose the decision variable has k -dimensions ($\chi = (\chi_1, \dots, \chi_k)$) and the variable in dimension i has m_i possible values. Denote M as the maximum m_i for all i , and the feasible region can be divided into M^k areas. The action probability vector can be expressed by a $k \times M$ matrix, $P_n(k \times M)$, at the n^{th} iteration, where:

$$P_1(i, j) = \begin{cases} \frac{1}{m_i} & j = 1, 2, 3, \dots, m_i \\ 0 & j > m_i \quad i = 1, 2, \dots, k \end{cases} \quad (40)$$

In the master problem, for example, if there are 2 candidate nodes and the capacity can be 100kW, 200kW and 300kW in the first level model, then $P_n(k \times M)$ is initialized as:

$$P_{allo,1}(k \times M) = \begin{bmatrix} 1/2 & 1/2 & 0 \\ 1/3 & 1/3 & 1/3 \\ 1/2 & 1/2 & 0 \\ 1/3 & 1/3 & 1/3 \end{bmatrix} \quad (41)$$

$P_{allo,1}(1,1)$ and $P_{allo,1}(1,2)$ are the possibility that there is and there isn't a RDG in candidate node 1 respectively. $P_{allo,1}(2,1)$, $P_{allo,1}(2,2)$ and $P_{allo,1}(2,3)$ are the possibility that the capacity of RDG in node 1 is 100kW, 200kW and 300kW respectively. The decision that "a 200kW RDG is located in node 1 and no RDG is located in node 2" is a feasible solution in the solution space, and the possibility that this solution is selected by the automaton is $P_{allo,1}(1,1) \times P_{allo,1}(2,2) \times P_{allo,1}(3,2) = 1/12$.

In the slave problem, for example, there are 3 loops in the network and there are 3, 5 and 4 switches in the loops respectively, then the vector for can be initialized as:

$$P_{conf,1}(k \times M) = \begin{bmatrix} \dots \\ 1/3 & 1/3 & 1/3 & 0 & 0 \\ 1/5 & 1/5 & 1/5 & 1/5 & 1/5 \\ 1/4 & 1/4 & 1/4 & 1/4 & 0 \\ \dots \end{bmatrix} \quad (42)$$

This 3 rows correspond to one configuration vector in the dynamic reconfiguration control variable.

(2) Step 2: Initialize the optimal value $best_1$. Set ξ to be its expected value. The optimal value of master problem

$best_{allo,1}$ is assigned to be the annual cost without considering RDG penetration or network reconfiguration. For the slave problem, the optimal value $best_{conf,1}$ is assigned to be the annual operation cost considering RDG allocation and RDG power control strategy, but not considering network reconfiguration.

(3) Step 3: Generate a set of random environment variables ξ_n randomly according to the probability distributions respectively.

(4) Step 4. Generate a set of control actions χ_n randomly based on $P_n(k \times M)$.

(5) Check the constraints and calculate the value of the objective functions $f_{obj}(\chi_n, \xi_n)$. The variable $FLAG$ is a symbol of whether the constraints are satisfied, defined as:

$$FLAG = \begin{cases} 1 & \text{when no constraint is violated} \\ 0 & \text{otherwise} \end{cases} \quad (43)$$

Calculate the response of the environment using:

$$\beta(\chi_n) = \begin{cases} \exp(-\frac{best_n}{f_{obj}(\chi_n, \xi_n)}), & \text{if } FLAG(\chi_n) = 1 \\ 1, & \text{if } FLAG(\chi_n) = 0 \end{cases} \quad (44)$$

where, $best_n$ the is current optimal value of the objective function. The designation of the reinforcement formula is based on 3 concerns: $\beta \in (0,1)$, β is continuous, and β is monotonically increasing with f_{obj} .

(6) Update the probability distributions of the decision actions.

For the values that χ_i ($i = 1 \dots n$) are selected, the probabilities are updated by using:

$$P_{n+1}(i, j) = \begin{cases} P_n(i, j) + a_f \cdot (e^{-1} - \beta(\chi_n))\beta(\chi_n) < e^{-1} \\ P_n(i, j)\beta(\chi_n) \geq e^{-1} \end{cases} \quad (45)$$

For the other intervals, the probabilities are updated by using:

$$P_{n+1}(i, j) = \begin{cases} P_n(i, j) - \frac{a_f \cdot (e^{-1} - \beta(\chi_n))}{m_i - 1} & j \leq m_i \text{ and } \beta(\chi_n) < e^{-1} \\ P_n(i, j) & j > m_i \text{ or } \beta(\chi_n) \geq e^{-1} \end{cases} \quad (46)$$

where, a_f is a constant parameter.

(7) Update the current optimal value of objective function.

$$best_{n+1} = \begin{cases} f(\chi_n, \xi_n) & \beta(\chi_n) < e^{-1} \\ best_n & \beta(\chi_n) \geq e^{-1} \end{cases} \quad (47)$$

(8) Terminate condition:

The optimization process ends when (48) or (49) is satisfied:

$$n \geq N_{iteration} \quad (48)$$

$$\gamma(n) = \min_i \max_j P_n(i, j) \geq \gamma_0 \quad (49)$$

where, $N_{iteration}$ is the maximum iterations, γ_0 is a constant number. Eq. (49) means there is a high enough possibility (more than γ_0^k) that a certain solution (the optimization result) in the feasible region will be selected by the automaton.

(9) Return the results: for each dimension of the control variable, the value with maximum probability is returned as the result. The annual cost (total cost in the master problem, operation cost in the slave problem) is returned as the fitness of the control variable.

B. POWER CONTROL STRATEGIES IN THE THIRD LEVEL

The principle of the RDG power control strategy is to maximize the renewable energy consumption under the system constraints. In distribution system, the voltage over-limit is the most significant problem which generally occurs before the current over-limit. So, this strategy considers two situations when the voltage constraint might be violated:

(1) The output of RDG is too high that the voltage magnitudes of the nodes where RDGs are allocated exceed the upper limit.

(2) With the load growth, the minimum voltage magnitude of the network exceeds the lower limit.

```

1 All the RDGs operate under the MPPT condition
2 flag_control=1
3 Calculate the voltage profile by Distflow equations
4 While Voltage exceeds the upper limit
   Curtail the active power of the RDG in the node
   with maximum voltage magnitude
5 End
6 While Voltage exceeds the lower limit
7   If The equal sign of constraint Eq. (35) has been
   reached for all RDGs
   flag_control=0
   Return
8   Else
   (1) Define v_m: the node with minimum voltage magnitude
   (2) Define Ω_re: The nodes with RDGs which have reactive power
   margin
   (3) Calculate the sensitivities between the voltage magnitude
   of node v_m and the injected reactive power of the nodes in Ω_re
   (4) Increase the reactive power of the RDG connected with the
   node in Ω_re which has the maximum sensitivity, until the
   voltage constraint is satisfied or the equal sign of constraint Eq.
   (35) has been reached
9   End
   Go to Step 3
10 End
    
```

FIGURE 3. Pseudo code of the RDG power control strategy.

Based on this consideration, a MPPT based strategy considering active power curtailment and reactive power compensation is given in this paper. The pseudo code of the strategy is shown in Fig. 3. It should be noted that the stochastic characteristics of renewable energy and loads have been dealt with in the FALA based algorithms. In the third level, the strategy is faced with a deterministic environment.

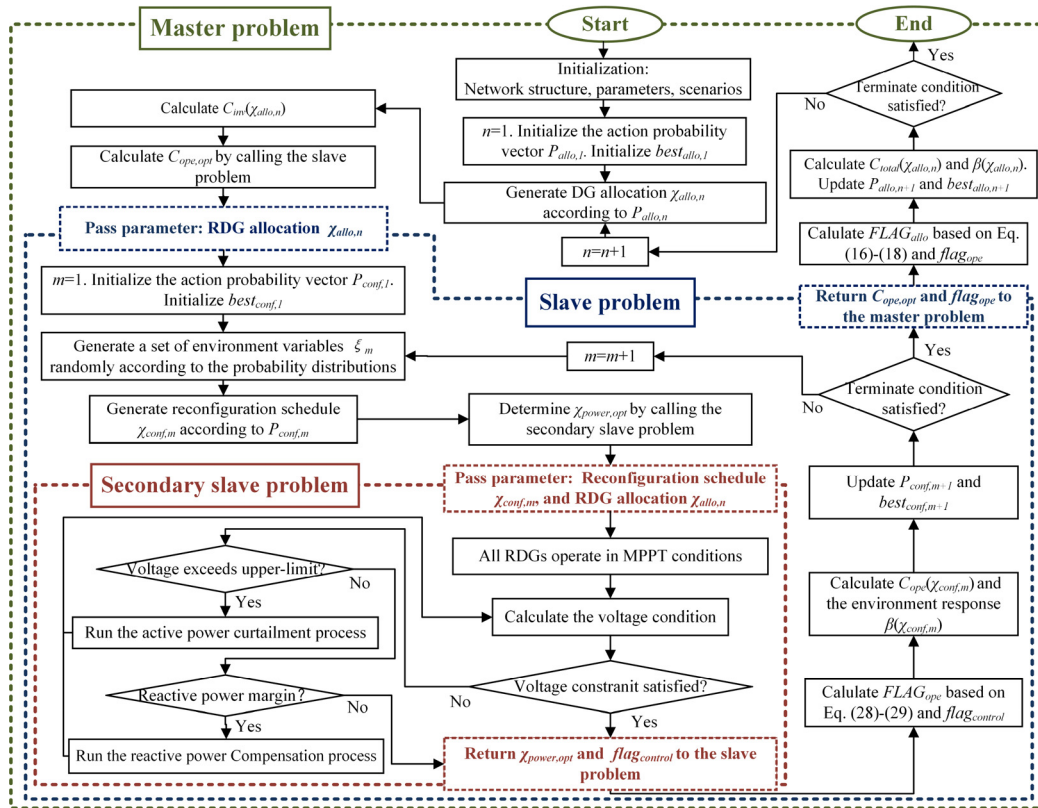


FIGURE 4. The entire solving process of the 3-level model.

C. THE ENTIRE SOLVING PROCESS OF THE 3-LEVEL MODEL

The entire process of the simultaneous algorithm to solve the 3-level model is shown in Fig. 4. The logical structure of 3 levels is the same with Fig. 1. The stochastic characteristics of renewable energy and loads are dealt with in the slave problem.

IV. CASE STUDY

A. PARAMETER SETTINGS

The proposed method is demonstrated in the 33-bus [27] and 69-bus [32] distribution test systems. The planning horizon is 10 years. Spring, summer, autumn and winter are considered as 4 typical scenarios in a year, and the mean value of the daily profiles of residential load and commercial load in a real distribution system [33] are used to represent the load characteristics in 4 scenarios, as shown in Fig. 5.

Photovoltaic (PV) is considered as the renewable energy, and the daily PV output profiles in 4 seasons are provided in Table 1 [34]. The PV output in summer is based on the statistical data and is multiplied by coefficients to generate the output profiles in other seasons. The loads in buses 37, 38 and 48 of the 33-bus system and the load in buses 37, 38 and 48 of the 69-bus system are set as commercial loads and others are set as residential loads. The standard deviations in normal distributions of PV and load are all set to be 10% of the

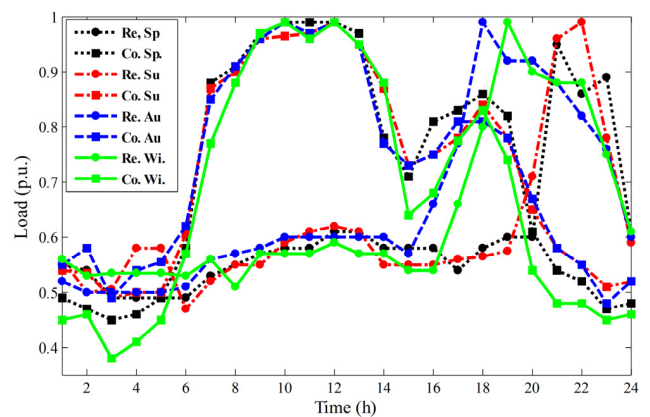


FIGURE 5. Power profile (in percentage of peak) for residential (Re.) and commercial (Co.) loads, in spring (Sp.), summer (Su.), autumn (Au.), and winter (Wi.)

expected value. The parameters in FALA are set as follows: $a_f = 7$; $N_{iteration} = 100$; $\gamma_0 = 0.8$.

Other parameters are listed in Table 2.

For each test system the optimization results or operation status of following cases are compared:

Case 1: The original systems without considering RDG penetration or network reconfiguration. There is no optimization process in this case. A note is that in this case the voltage

TABLE 1. Daily PV output in 4 seasons as a fraction of yearly peak.

| Time | Spring PV output | Summer PV output | Autumn PV output | Winter PV output |
|-------|---------------------|---------------------|---------------------|---------------------|
| 1-7 | 0 | 0 | 0 | 0 |
| 8 | 0.0433 | 0.0476 | 0.0424 | 0.0381 |
| 9 | 0.2167 | 0.2381 | 0.2119 | 0.1905 |
| 10 | 0.4333 | 0.4762 | 0.4238 | 0.3810 |
| 11 | 0.6933 | 0.7619 | 0.6781 | 0.6095 |
| 12 | 0.7800 | 0.8571 | 0.7629 | 0.6857 |
| 13 | 0.8667 | 0.9524 | 0.8476 | 0.7619 |
| 14 | 0.9100 | 1 | 0.8900 | 0.8000 |
| 15 | 0.8233 | 0.9048 | 0.8052 | 0.7238 |
| 16 | 0.6500 | 0.7143 | 0.6357 | 0.5714 |
| 17 | 0.4333 | 0.4762 | 0.4238 | 0.3810 |
| 18 | 0.2167 | 0.2381 | 0.2119 | 0.1905 |
| 19 | 0.0867 | 0.0952 | 0.0848 | 0.0762 |
| 20-24 | 0 | 0 | 0 | 0 |

TABLE 2. Parameters in the case study.

| Parameters | Values |
|--------------------------------|--|
| RDG 33-bus system | Buses 11-18 and Buses 31-33 |
| Candidate nodes 69-bus system | Buses 21-27 and Buses 50-54 |
| RDG base unit | 100kV·A |
| Load growth | 2%/year |
| RDG installation cost: | \$50000+\$1100/kV·A |
| RDG O&M cost c_{om} | 15\$/(kV·A·year) |
| Electricity price c_{uti} | Peak time 0.082\$/kW·h Valley time 0.049\$/kW·h |
| Reconfiguration cost c_{rec} | 0.083\$ |
| compensation price c_{sub} | 0.04\$/kW·h |
| $[V_{min}, V_{max}]$ | [0.9, 1.05] |

constraints (36) will not be satisfied in the 33-bus or 69-bus systems since the 8th and 7th year respectively because of the load growth.

Case 2: The optimal siting and sizing of RDG are considered, but the network reconfiguration is not considered. The modeling of this case is modified from proposed model: in the second stage of the master—slave structure, the optimization of χ_{conf} is omitted. χ_{conf} is set to be constant so that the network structure is not reconfigured.

Case 3: Both the optimal siting and sizing of RDG and the dynamic network reconfiguration are considered. Proposed model, algorithm and strategy are applied to solve the problem in this case.

B. RESULTS OF RDG ALLOCATION AND RECONFIGURATION STRATEGY

The optimal RDG allocation in Case 2, 3 and the network reconfiguration strategy in Case 3 are shown in Table 3-6. According to Table 3 and Table 5, in the 33-bus and 69-bus systems the optimal capacity of PVs in Case 3 are 34% and 30% higher than that in Case 2 respectively. According to Table 4 and Table 6, the network reconfiguration occurs mostly in 10:00-15:00, when the maximum output of PVs is relatively high.

TABLE 3. RDG location and capacity in the 33-bus system.

| Bus Number | Capacity | |
|------------|----------|---------|
| | Case 2 | Case 3 |
| Bus 12 | | 1500 kW |
| Bus 17 | 1300kW | 1100 kW |
| Bus 30 | 1100kW | |
| Bus 31 | | 1700 kW |
| Bus 33 | 800kW | |

TABLE 4. Network reconfiguration schedule of the 33-bus system in case 3.

| Scenarios | Time | Operation |
|-----------|-------|--------------------------------|
| Spring | 9:00 | close s36, s37, open s3, s8 |
| | 11:00 | close s35, open s12 |
| | 16:00 | close s12, open s35 |
| | 17:00 | close s3, s8, open s36, s37 |
| Summer | 8:00 | close s37, open s24 |
| | 10:00 | close s35, s36 open s2, s16 |
| | 17:00 | close s24, open s37 |
| | 19:00 | close s16, s2, open s35, s36 |
| Autumn | 9:00 | close s37, open s28 |
| | 11:00 | close s35, open s2 |
| | 17:00 | close s2, s28, open s35, s37 |
| Winter | 12:00 | close s34, s35, open s2, s12 |
| | 16:00 | close s2, s12, opens s34, s35; |

TABLE 5. RDG location and capacity in the 69-bus system.

| Bus Number | Capacity | |
|------------|----------|---------|
| | Case 2 | Case 3 |
| Bus 21 | 700 kW | |
| Bus 22 | | 800 kW |
| Bus 27 | 900 kW | 1200 kW |
| Bus 50 | 1400 kW | |
| Bus 51 | | 1300 kW |
| Bus 53 | | 600 kW |

C. ECONOMIC AND TECHNICAL ANALYSIS

The results of Case 1-3 are analyzed and compared on aspect of economic benefit, RDG consumption and power loss. Table 7 and Table 8 show the detailed result of investment and operation costs.

In the 33-bus system, the total annual cost in Case 3 is 7.27% less than that in Case 2, and in the 69-bus system this proportion is 6.74%. The penetration of PV can reduce the system total cost by 15-18% when network reconfiguration is not considered and by 21%-24% when considering network reconfiguration, respectively. The benefits are mostly caused by government compensation, however, with development of PV technology, price reduction of PV modules and extension of PV life cycle and planning horizon, the economic advantage of PV will gradually show.

The PV energy consumption and curtailment data is shown in Table 9. According to Table 9, there is a significant growth in the renewable energy consumption when considering

TABLE 6. Network reconfiguration schedule of the 69-bus system in case 3.

| Scenarios | Time | Operation |
|-----------|-------|---|
| Spring | 8:00 | close s70, open s17, |
| | 10:00 | close s71, open s5 |
| | 12:00 | close s72, open s43 |
| | 16:00 | close s5, s43, open s71, s72 |
| | 17:00 | close s17, open s70 |
| Summer | 10:00 | close s72, s73, open s53, s43 |
| | 12:00 | close s69,s70, s71 open s7, s67, s17 |
| | 16:00 | close s17, s53, s43, open s70; s73; s72 |
| | 18:00 | close s67, open s71 |
| | 19:00 | close s7, open s69 |
| Autumn | 9:00 | close s73, open s11 |
| | 10:00 | close s71, s72, open s58 s5 |
| | 16:00 | close s58, s5, open s71, s72 |
| | 18:00 | close s11, open s73 |
| Winter | 10:00 | close s72, open s47 |
| | 12:00 | close s71, open s4 |
| | 16:00 | close s4, s47, open s71, s72; |

TABLE 7. Economic analysis of the 33-bus case.

| | Case 1 | Case 2 | Case 3 |
|-------------|-------------------|-------------------|-------------------|
| C_{cap} | / | 342,991 \$/year | 456,075 \$/year |
| C_{uti} | 1,326,670 \$/year | 912,385 \$/year | 776,673 \$/year |
| C_{ope} | C_{om} | / | 33,713 \$/year |
| | C_{rec} | / | / |
| | C_{sub} | / | 199 \$/year |
| | C_{sub} | / | 200,511 \$/year |
| C_{total} | 1,326,670 \$/year | 1,088,577 \$/year | 1,009,422 \$/year |

TABLE 8. Economic analysis of the 69-bus case.

| | Case 1 | Case 2 | Case 3 |
|-------------|-------------------|-------------------|-------------------|
| C_{cap} | / | 322,429 \$/year | 419,626 \$/year |
| C_{uti} | 1,387,971 \$/year | 1,006,496 \$/year | 881,708 \$/year |
| C_{ope} | C_{om} | / | 31,606 \$/year |
| | C_{rec} | / | / |
| | C_{sub} | / | 182,922 \$/year |
| | C_{sub} | / | 244,355 \$/year |
| C_{total} | 1,387,971 \$/year | 1,177,609 \$/year | 1,098,265 \$/year |

TABLE 9. Renewable energy consumption analysis.

| Renewable Energy consumption and curtailment | Case 1 | Case 2 | Case 3 |
|--|-------------|--------|----------------|
| 33-bus syster | Consumption | / | 7.17 GW·h/year |
| | Curtailment | / | 74.1 MW·h/year |
| 69-bus syster | Consumption | / | 6.72 GW·h/year |
| | Curtailment | / | 67.7 MW·h/year |

network reconfiguration, however, there is still similar amount of energy curtailment even in Case 3. That’s because the optimization process always leads to the balance that the marginal benefit caused by the unit capacity is equal to the marginal cost, and a level of energy curtailment is the essential condition of this situation. However, the total

capacity of PVs and the renewable energy consumed by the system have increased significantly (about 30%-34%) when network reconfiguration is considered. The curtailment occurs during 12:00-15:00, and the proportion of curtailment in summer is 78%. The detailed distribution of renewable energy curtailment is shown in Fig. 6(a)-(d).

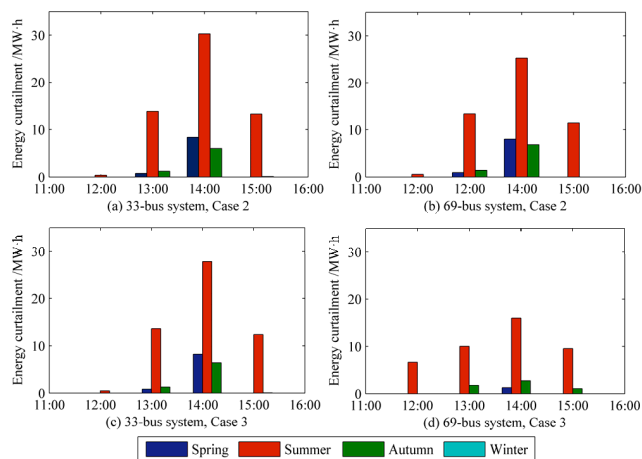


FIGURE 6. The distribution of renewable energy curtailment.

TABLE 10. Annual power losses.

| Power loss | Case 1 | Case 2 | Case 3 |
|---------------|---------------|---------------|---------------|
| 33-bus system | 850 MW·h/year | 787 MW·h/year | 849 MW·h/year |
| 69-bus system | 949 MW·h/year | 831 MW·h/year | 800 MW·h/year |

The annual power losses of the system in three cases is shown in Table 10. The analysis is on following aspects:

(1) The power loss is depend on the current magnitude and the resistance of the lines in the network;

(2) The power losses of the systems with RDG penetration is not decreased compared with the original network, because the power from RDG to loads also causes line loss in the periods when the output of RDG is high.

(3) For a certain system, the network reconfiguration can balance the line power and reduce power loss. However, the total RDG capacity in 3 cases are not the same, so the power loss reduction caused by network reconfiguration cannot be reflected in Table 10.

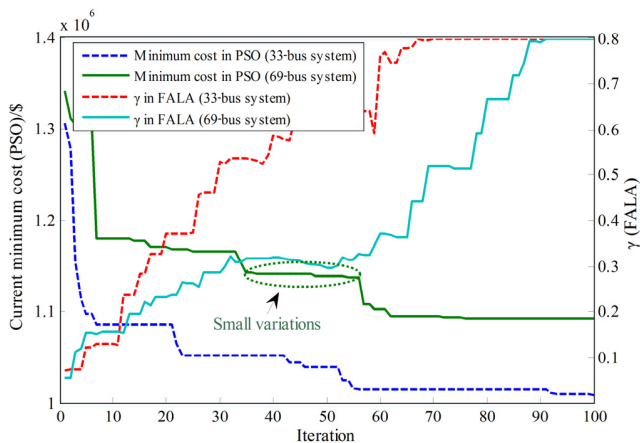
(4) The reactive power compensation in the third level is a strategy to help satisfy the voltage constraints, while the compensation power is not optimized precisely considering model complexity, and the reactive power compensation ability of the RDG is not totally used. A simple test is given by increase the lower limit of voltage magnitude. When the lower limit is set as 0.92, the annual power loss of the 33-bus and 69-bus systems in Case 3 will be 792 MW·h and 725 MW·h respectively. The loss will get higher again if keeping increasing the lower limit because the active power flow from the RDG to loads will increase the current magnitude.

TABLE 11. Performance of FALA and PSO algorithms.

| | 33-bus system | | 69-bus system | |
|------------------|---------------|--------------|---------------|--------------|
| | FALA | PSO | FALA | PSO |
| Calculating time | 82 min | 12h 48min | 136 min | 19h 15min |
| Annual cost | 1,009,422 \$ | 1,007,604 \$ | 1,098,265 \$ | 1,109,067 \$ |
| RDG penetration | 4300 kW | 4200 kW | 3900 kW | 3700 kW |

D. ALGORITHM ANALYSIS

To demonstrate the effectiveness and applicability of proposed algorithm, the particle swarm optimization (PSO) algorithm which has been widely used is also applied in Case 3. The comparison between FALA based algorithm and PSO algorithm is shown in Table 11. In Case 3, the first level and second level control variables need to be optimized, and the second level process is called in each iteration of the first level optimization. Considering the stochastic characteristics of PV and loads, the sampling method (e.g., chance constrained programming) should also be introduced if applying PSO algorithm in the second level, leading the total calculating time unacceptable (more than 48 hours) or even memory overflow. So in this comparison the PSO is only applied in the first level model and the second level is still optimized by FALA based algorithm. In the PSO, the pop population is set as 20 and the number of total iteration times is set as 100.

**FIGURE 7. Convergence process of FALA and PSO algorithms.**

The convergence process is shown in Fig. 7. γ is defined in Eq. (49). γ is not monotone increasing because it is possible that in some dimension the control variable is not generated as the “most probable one” while the fitness value of the control variable is current optimal, which may lead the γ updated smaller (seen Eq. (44)- (46)). In the 33-bus and 69-bus systems the FALA based algorithm converges after 67 and 91 iterations respectively. The computing time of PSO algorithm is much longer than that of FALA algorithm, while there is no significant difference between 2 algorithms on the aspect of searching capability: in the 33-bus system the result of PSO algorithm is better while in the 69-bus system the result of FALA algorithm is better, and both of the gaps

are very small. So we can draw the conclusion that FALA algorithm is more efficient in proposed model.

The PSO convergence curves are not very typical because there are some small variations in “current minimum cost”, seen in Fig. 7. For example, during 34-56 iteration the current minimum cost in PSO optimization for the 69-bus system is changed slightly for several time while the current optimal solution (capacity and location variable information) is not changed. That’s because the objective function calculation of current optimal solution calls the second level FALA based algorithm each iteration to determine the reconfiguration schedule, and the result could be different since the FALA optimization is a stochastic process.

V. CONCLUSION

In this paper, an optimal RDG siting and sizing method considering network reconfiguration and RDG power control strategy is proposed. A 3-level iterative master—slave structure is established following the order of RDG planning and distribution system operation. Considering the model complexity, a practical strategy is given to determine the RDG power in the secondary slave problem, while the RDG allocation in the master problem and reconfiguration schedule optimization in the slave level are solved by learning automata based algorithms which can deal the stochastic characteristics of load and renewable energy.

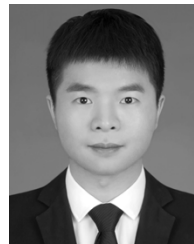
Results shows that the optimal capacity of the RDG is increased and higher economic benefits can be achieved if network reconfiguration is considered in the system operation stage, and that proposed learning automata based algorithms have higher optimizing efficiency compared with conventional intelligent algorithm.

In future work, the automation level of distribution systems and the relay protection system which may add constraints of the network reconfiguration and RDG power control should be taken into consideration. On the other hand, proposed RDG allocation model has reference meaning for switch placement and expansion planning of future active distribution systems with high penetration of RDG.

REFERENCES

- [1] S. N. G. Naik, D. K. Khatod, and M. P. Sharma, “Analytical approach for optimal siting and sizing of distributed generation in radial distribution networks,” *IET Gener. Transm. Distrib.*, vol. 9, no. 3, pp. 209–220, Feb. 2015.
- [2] K. M. Muttaqi et al., “Optimizing distributed generation parameters through economic feasibility assessment,” *Appl. Energy*, vol. 165, pp. 893–903, Mar. 2016.
- [3] J. Mitra, M. R. Vallem, and C. Singh, “Optimal deployment of distributed generation using a reliability criterion,” *IEEE Trans. Ind. Appl.*, vol. 52, no. 3, pp. 1989–1997, May/Jun. 2016.
- [4] M. Rahmani-Andebili, “Distributed generation placement planning modeling feeder’s failure rate and customer’s load type,” *IEEE Trans. Ind. Electron.*, vol. 63, no. 3, pp. 1598–1606, Mar. 2016.
- [5] Z. Liu, F. Wen, and G. Ledwich, “Optimal siting and sizing of distributed generators in distribution systems considering uncertainties,” *IEEE Trans. Power Del.*, vol. 26, no. 4, pp. 2541–2551, Oct. 2011.
- [6] B. R. Pereira, G. R. M. D. Costa, and J. Contreras, “Optimal distributed generation and reactive power allocation in electrical distribution systems,” *IEEE Trans. Sustain. Energy*, vol. 7, no. 3, pp. 1–10, Jul. 2016.

- [7] Y. Aliari and A. Haghani, "Planning for integration of wind power capacity in power generation using stochastic optimization," *Renew. Sustain. Energy Rev.*, vol. 59, pp. 907–919, Jun. 2016.
- [8] G. Carpinelli *et al.*, "Optimisation of embedded generation sizing and siting by using a double trade-off method," *Proc. Inst. Electr. Eng.—Gener., Transm. Distrib.*, vol. 152, no. 4, pp. 503–513, Jul. 2005.
- [9] G. Celli, E. Ghiani, S. Mocci, and F. Pilo, "A multiobjective evolutionary algorithm for the sizing and siting of distributed generation," *IEEE Trans. Power Syst.*, vol. 20, no. 2, pp. 750–757, May 2005.
- [10] C. C. Chu and M. S. Tsai, "Application of novel charged system search with real number string for distribution system loss minimization," *IEEE Trans. Power Syst.*, vol. 28, no. 4, pp. 3600–3609, Nov. 2013.
- [11] Y.-L. Ke, C.-S. Chen, M.-S. Kang, J.-S. Wu, and T.-E. Lee, "Power distribution system switching operation scheduling for load balancing by using colored Petri nets," *IEEE Trans. Power Syst.*, vol. 19, no. 1, pp. 629–635, Feb. 2004.
- [12] R. Yan and T. K. Saha, "Investigation of voltage imbalance due to distribution network unbalanced line configurations and load levels," *IEEE Trans. Power Syst.*, vol. 28, no. 2, pp. 1829–1838, May 2013.
- [13] B. Arandian, R. A. Hooshmand, and E. Gholipour, "Decreasing activity cost of a distribution system company by reconfiguration and power generation control of DGs based on shuffled frog leaping algorithm," *Int. J. Electr. Power Energy Syst.*, vol. 61, pp. 48–55, Oct. 2014.
- [14] A. M. Imran and M. Kowsalya, "A new power system reconfiguration scheme for power loss minimization and voltage profile enhancement using fireworks algorithm," *Int. J. Electr. Power Energy Syst.*, vol. 62, pp. 312–322, Nov. 2014.
- [15] F. Capitanescu *et al.*, "Assessing the potential of network reconfiguration to improve distributed generation hosting capacity in active distribution systems," *IEEE Trans. Power Syst.*, vol. 30, no. 1, pp. 346–356, Jan. 2015.
- [16] J. Zhu *et al.*, "An improved PSO algorithm based on statistics for distribution network reconfiguration to increase the penetration of distributed generations," in *Proc. IET Int. Conf. Resilience Transm. Distrib. Netw. (RTDN)*, Jul. 2015, pp. 1–6.
- [17] C. Lueken, P. M. Carvalho, and J. Apt, "Distribution grid reconfiguration reduces power losses and helps integrate renewables," *Energy Policy*, vol. 48, pp. 260–273, Sep. 2012.
- [18] G. Gutiérrez-Alcaraz, E. Galván, N. González-Cabrera, and M. S. Javadi, "Renewable energy resources short-term scheduling and dynamic network reconfiguration for sustainable energy consumption," *Renew. Sustain. Energy Rev.*, vol. 52, pp. 256–264, Dec. 2015.
- [19] M. E. H. Golshan and S. A. Arefifar, "Distributed generation, reactive sources and network-configuration planning for power and energy-loss reduction," *Proc. Inst. Electr. Eng.—Gener., Transm. Distrib.*, vol. 153, no. 2, pp. 127–136, Mar. 2006.
- [20] F. Ding and K. A. Loparo, "Feeder reconfiguration for unbalanced distribution systems with distributed generation a hierarchical decentralized approach," *IEEE Trans. Power Syst.*, vol. 31, no. 2, pp. 1633–1642, Mar. 2016.
- [21] R. S. Rao, K. Ravindra, K. Satish, and S. V. L. Narasimham, "Power loss minimization in distribution system using network reconfiguration in the presence of distributed generation," *IEEE Trans. Power Syst.*, vol. 28, no. 1, pp. 317–325, Feb. 2013.
- [22] A. M. Imran, M. Kowsalya, and D. P. Kothari, "A novel integration technique for optimal network reconfiguration and distributed generation placement in power distribution networks," *Int. J. Electr. Power Energy Syst.*, vol. 63, pp. 461–472, Dec. 2014.
- [23] T. T. Nguyen, A. V. Truong, and T. A. Phung, "A novel method based on adaptive cuckoo search for optimal network reconfiguration and distributed generation allocation in distribution network," *Int. J. Electr. Power Energy Syst.*, vol. 78, pp. 801–815, Jun. 2016.
- [24] H. B. Tolabi, M. H. Ali, and M. Rizwan, "Simultaneous reconfiguration, optimal placement of DSTATCOM, and photovoltaic array in a distribution system based on fuzzy-ACO approach," *IEEE Trans. Sustain. Energy*, vol. 6, no. 1, pp. 210–218, Jan. 2015.
- [25] A. Zidan, M. F. Shaaban, and E. F. El-Saadany, "Long-term multi-objective distribution network planning by DG allocation and feeders' reconfiguration," *Electr. Power Syst. Res.*, vol. 105, pp. 95–104, Dec. 2013.
- [26] M. Esmaili, M. Sedighzadeh, and M. Esmaili, "Multi-objective optimal reconfiguration and DG (distributed generation) power allocation in distribution networks using big bang-big crunch algorithm considering load uncertainty," *Energy*, vol. 103, pp. 86–99, May 2016.
- [27] M. E. Baran and F. F. Wu, "Network reconfiguration in distribution systems for loss reduction and load balancing," *IEEE Trans. Power Del.*, vol. 4, no. 2, pp. 1401–1407, Apr. 1989.
- [28] J. M. Harris, J. L. Hirst, and M. J. Mosinghoff, *Combinatorics and Graph Theory*, vol. 2. New York, NY, USA: Springer, 2008.
- [29] Y. Wu, R. Lu, and P. Shi, "Adaptive output synchronization of heterogeneous network with an uncertain leader," *Automatica*, vol. 76, pp. 183–192, Feb. 2017.
- [30] Y. Wu *et al.*, "Consensus of multiagent systems using aperiodic sampled-data control," *IEEE Trans. Cybern.*, vol. 46, no. 9, pp. 2132–2143, Sep. 2016.
- [31] M. A. L. Thathachar and P. S. Sastry, "Varieties of learning automata: An overview," *IEEE Trans. Syst., Man, Cybern.*, vol. 32, no. 6, pp. 711–722, Dec. 2002.
- [32] M. E. Baran and F. F. Wu, "Optimal capacitor placement on radial distribution systems," *IEEE Trans. Power Del.*, vol. 4, no. 1, pp. 725–734, Jan. 1989.
- [33] P. Poonpun and W. T. Jewell, "Analysis of the cost per kilowatt hour to store electricity," *IEEE Trans. Energy Convers.*, vol. 23, no. 2, pp. 529–534, Jun. 2008.
- [34] S. Wilcox. National solar radiation database 1991–2010 update. National Renewable Energy Laboratory (NREL), U.S. Department of Energy, Washington, DC, USA, accessed on Jul. 2017. [Online]. Available: http://redc.nrel.gov/solar/old_data/nsrdb/1991-2010/



JUNPENG ZHU received the B.S. degree in applied mathematics from Southeast University, China, in 2012, where he is currently pursuing the Ph.D. degree with the School of Electrical Engineering. His research interests include distributed generations integration, optimization, and control of active distribution networks.



WEI GU (M'06–SM'16) received the B.S. and Ph.D. degrees in electrical engineering from Southeast University, China, in 2001 and 2006, respectively. From 2009 to 2010, he was a Visiting Scholar with the Department of Electrical Engineering, Arizona State University, Tempe, AZ, USA. He is currently a Professor with the School of Electrical Engineering, Southeast University. He is also the Director with the Institute of Distributed Generations and Active Distribution Networks. His research interests include distributed generations and microgrids, active distribution networks.



GUANNAN LOU received the B.S. and M.S. degrees in control science and engineering from North China Electric Power University, China, in 2008 and 2011, respectively. She is currently pursuing the Ph.D. degree with the School of Electrical Engineering, Southeast University, China. From 2011 to 2015, she was with Guodian Nanjing Automation Co., Ltd, Nanjing. Her research interests include distributed generations integration, microgrid modeling, control, and optimization.

LIUFANG WANG is currently with the State Grid Anhui Electric Power Corporation Research Institute, Hefei, China. His research interests include active distribution network and power system operation.

BIN XU is currently with the State Grid Anhui Electric Power Corporation Research Institute, Hefei, China. His research interests include active distribution network and power system operation.

MING WU received the Ph.D. degree from the University of Chinese Academy of Sciences. He is currently with the China Electric Power Research Institute, Beijing, China. His research interests are about microgrid control and renewable energy integration.

WANXING SHENG received the B.S., M.S., and Ph.D. degrees from Xi'an Jiaotong University, Xi'an, China. Since 1997, he has been a Full Professor with the China Electric Power Research Institute, Beijing, China, where he is currently the Head of the Department of Power Distribution. He is also the Leader with the Intelligent Distribution Power System and an Excellent Expert of State Grid Corporation of China. He has authored over 150 refereed journal and conference papers, and 15 books. His research interests include power system analysis and automation, renewable energy, and smart grid integration. He has also completed numerous state-funded research and development projects as a Principal Investigator.

• • •